

# INTERNATIONAL SOCIETY FOR SOIL MECHANICS AND GEOTECHNICAL ENGINEERING



*This paper was downloaded from the Online Library of the International Society for Soil Mechanics and Geotechnical Engineering (ISSMGE). The library is available here:*

<https://www.issmge.org/publications/online-library>

*This is an open-access database that archives thousands of papers published under the Auspices of the ISSMGE and maintained by the Innovation and Development Committee of ISSMGE.*

# Slope stabilisation in earthquake prone environment – with a flexible high-tensile steel chain-link mesh

## Stabilisation de pente dans un milieu propice aux séismes – avec un filet flexible en acier à haute limite élastique

H. Hofmann

*Geobrugg AG, Romanshorn, Switzerland*

A. Roduner

*Geobrugg AG, Romanshorn, Switzerland*

E. Gröner

*Geobrugg AG, Romanshorn, Switzerland*

**ABSTRACT:** In the last ten years only, several thousand earthquakes above a magnitude of 6 have occurred worldwide (USGS). With urbanisation growing incessantly, the risk to people and the damage to infrastructure from seismic events is increasing. The importance of including the seismic load case for building construction and retrofitting has long been recognised and is implemented around the world. Infrastructure protection against natural hazards, such as snow, rock and landslides, should as well take seismicity into account. The reaction force onto the subsystem is dependent of weight and absolute acceleration. A stiffer system therefore can be easier accelerated than a flexible, light, system, and will sustain more damage, such as buckling, shearing and cracking. The less protection measures weigh and the more flexible they are, the less is the risk of a failure. This paper presents three case studies, in Japan, Chile and the US, where flexible high tensile steel wire meshes for slope stabilization were successfully engaged while for example shotcrete grating crib works, right next to the flexible systems, failed. Different type of mesh systems exist, this contribution will only take into account the Tecco system developed by our company. Finally, it is explained how the dimensioning software Ruvolum for Tecco Slope Stabilization is taking the seismic load case into account.

**RÉSUMÉ:** Au cours des dix dernières années seulement, des milliers de séismes d'une magnitude supérieure à 6 se sont produits dans le monde (USGS). Avec l'urbanisation croissante, les risques pour la population et les dommages causés aux infrastructures par les séismes augmentent. L'importance d'inclure le scénario de charge sismique pour la construction et la modernisation des bâtiments et mise en œuvre dans le monde entier. La protection des infrastructures contre les risques naturels, tels que les glissements de terrain, devrait également prendre en compte la sismicité. La force de réaction sur le système dépend du poids et de l'accélération absolue. Un système plus rigide peut donc être plus accéléré plus facilement qu'un système flexible, et subira plus de dommages. Plus les mesures de protection sont souples et légères, moins le risque de dommage est grand. Cet article présente trois études de cas, au Japon, au Chili et aux États-Unis, où des treillis flexibles en acier à haute résistance à la traction pour la stabilisation des pentes ont été utilisés avec succès. Différents treillis existent pour la stabilisation de pente, dans ce cas nous allons seulement étudier le système Tecco développé par notre entreprise. Finalement, il est expliqué comment le système de dimensionnement Ruvolum pour le système Tecco prend en compte le cas de charge sismique.

**Keywords:** slope stabilisation, earthquakes, high-tensile steel chain-link mesh, flexible protection

## 1 INTRODUCTION

Earthquakes are defined as the shaking of the ground due to seismic waves travelling through, themselves triggered by the release of excess elastic strain accumulated in the bedrock. Earthquakes occur most often along major fault lines and therefore mostly at the boundary of tectonic plates. Approximately 50'000 noticeable earthquakes are recorded annually and of these, 100 cause severe damage when located close enough to inhabited areas (USGS n.d., Bolt, 2018).

Urbanized areas extend more and more their surfaces, subsequently the risk of damage by seismic activity is increasing. Visible effects of earthquakes on the ground are the damage of infrastructure and buildings and substantial geomorphological changes such as topographical changes, groundwater flow alteration, liquefaction of soils and trigger natural hazards such as landslides, rockslides and debris flows. In areas known to be prone for slope instabilities, an earthquake can increase the number of landslides substantially over several years after the earthquake by altering significantly the subsoil conditions (Clague and Stead, 2012). When these slopes are being stabilised by any type of protection or remediation measure, these should take into account the load case for earthquakes, such as the already existing standards for buildings, bridges etc ...

The latest large notable earthquakes, associated with the presented case studies further in these contribution, are the 2011  $M_w$ 9.1 Tohoku earthquake in Japan, the 2010,  $M_w$ 8.8 Bio-Bio earthquake in Chile and the 2011,  $M_w$ 5.8 Louisa earthquake in the United States. The first two earthquakes were due to thrust-faulting in the context of the subduction of the North American and Pacific plates and the Nazca and South

America plates ( “Poster M8.8 Maule Earthquake”, USGS; “Poster M9.1 Tohoku Earthquake”, USGS). The Louisa earthquake was of much less energy, occurring as a reverse fault, but was felt over a very large area, typical to the setting in the eastern US in contrast to the western US (“seismic hazards central Virginia”, USGS). This earthquake was additionally significant as it led to the revision of the US national seismic hazard map, since it was recognised that this was the largest earthquake in the eastern US since the start of recording and showed the potential for larger and more damaging earthquakes than previously considered (“update national seismic hazard map”, bdc network; “seismic hazard central virginia”, USGS; “nearly half americans exposed”, USGS; see Figure 1).

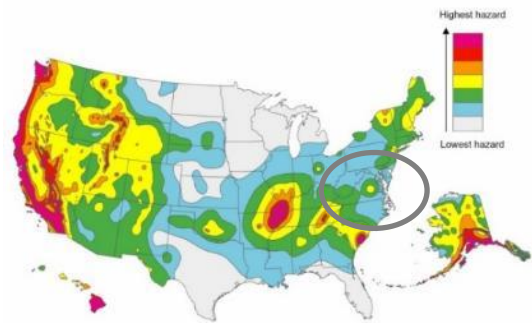


Figure 1: adapted seismic hazard map after the 2011  $M_w$ 5.8 Louisa earthquake (grey ellipse, USGS)

## 2 GROUND INSTABILITIES

Slope failures occur when the shear stress across a plane exceeds the strength of the substrate, which is quite a similar process to a fault rupture (Clague and Stead, 2012). Increase of the shear stress in the ground depends on multiple factors starting with the type of rock, type of underlying

rock, stratigraphy, state of weathering to the surrounding hydrogeology. The variation of temperature and precipitation, especially the alternation between extremes can then act as trigger for ground motion (Clague and Stead , 2012, and references therein) demonstrated the relationship between earthquakes and landslides. A strong ground motion associated with and already weakened hillslope will destabilise it, right away and years after. Several observations were made were a notable increase in landslides were recorded some years after in comparison to the movement rate before the earthquake. The rates of earthquake triggered landslides are

correlated with measured peak ground acceleration (PGA).

PGA represents the maximum ground acceleration occurring during an earthquake at a specific location. PGA is dependent on the local geology and not on the magnitude of the earthquake. PGA values are plotted on the seismic hazard maps and are expressed in  $m.s^{-2}$  or in g (“GSHAP”, ETHZ; Allen et al., 2008). The following Table 1 and Figure 2 show the PGA values for the three case study sites. Notice that the PGA value at the site in Chile is much higher than for the sites in Japan although the Japan earthquake was of larger magnitude.

Table 1: Typical peak ground acceleration values for case study earthquakes (Posters, USGS)

PGA (max recorded, $m.s^{-2}$ )	Magnitude	Earthquake
2.4 - 3.2	9.0	2011 Tohoku (Japan)
4 - 4.8	8.8	2010 Bio-Bio (Chile)
0.4-0.8	5.8	2011 Louisa (US)

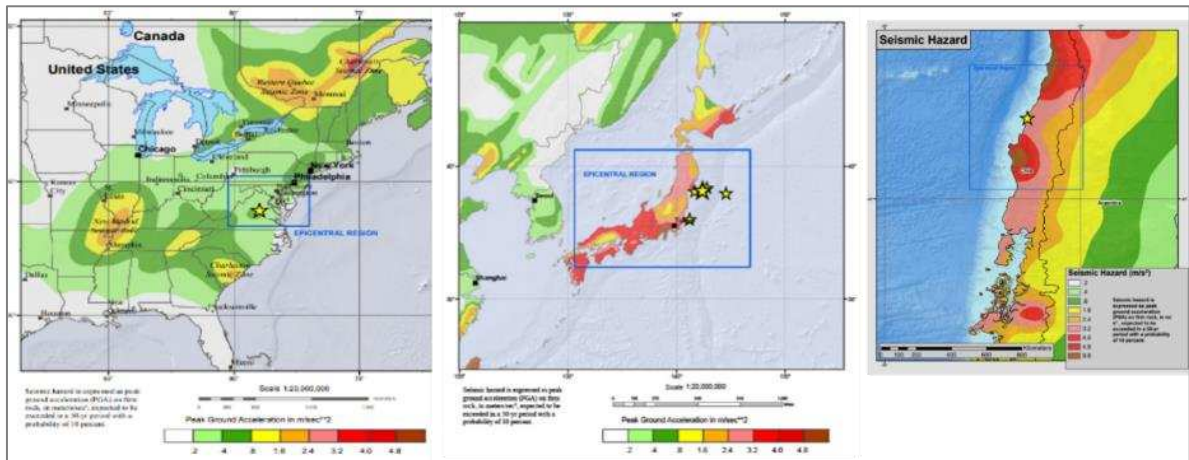


Figure 2: seismic hazard maps for the three case studies (Posters, USGS)

### 3 SLOPE STABILILITY MITIGATION

According to the European Norm EN 14490 (2010) three different type of facings exist for slope stabilisation purposes, divided into hard, soft and flexible.

#### 3.1 Hard facing

Hard facing corresponds generally to shotcrete or concrete structures. These systems generally don't fare well during an earthquake as the stiffer a structure is, the more it gets accelerated and

risks damage. Once damaged the protection measure loses its retention capacity.

### 3.2 Soft facing

Soft facings consist of different geogrids, geomembranes or geotextiles. This type is generally applied for temporary slope coverage, but wouldn't work during an earthquake. Although it is anything but stiff, the material presents a very low shear resistance and will tear with strong ground motion.

### 3.3 Flexible facing

Also defined as active slope stabilization systems, flexible facings are a combination of steel wire mesh with soil nailing. As the following case studies will show, a type of flexible facing, the Tecco system (high tensile steel wire mesh transmitting the forces of the slope acting on the mesh back into the ground via soil nails), from Geobrugg AG, supports well the peak ground acceleration during strong ground motion, as it can be dimensioned for (Cala et al., 2012).

### 3.4 Dimensioning of flexible facings

Slope stabilisation always starts with the dimensioning of the slope through the classical geotechnical calculations. This allows to get a nail grid spacing. Subsequently the flexible facing can be dimensioned with RUVOLUM, freely available software, to verify for shallow slope stability ( $\leq 2\text{m}$ ) and stability in between the nail grid. Both load cases are termed "sliding off parallel to the slope" and "local wedge-shaped rupture bodies". Additionally, the software does account for earthquake settings. The PGA values are split into a horizontal and vertical value ( $\varepsilon_h$  and  $\varepsilon_v$ ) and are taken into account in the equilibrium equation of both load cases mentioned above (see Figure 3). Detailed explanations can be found in Cala et al., 2012.

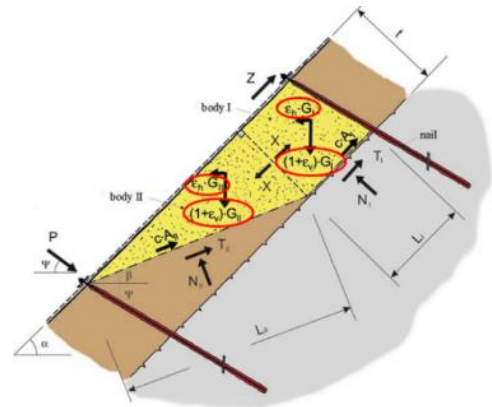


Figure 3: example of the PGA parameters  $\varepsilon_h$  and  $\varepsilon_v$  considered in the RUVOLUM software.

## 4 CASE STUDIES

Worldwide experience has been acquired in installing flexible high tensile steel wire mesh for slope stabilisation purposes, in quiet and in earthquake prone areas. Impressive examples of two of the largest earthquakes in the last 10 years and a third example are presented here, where the successful coping of the mesh with the ground shaking led to the successful retention of already failing slopes and avoided further damage.

### 4.1 Japan; Iwate Prefecture

On March 11<sup>th</sup> 2011, a magnitude 9.1 struck off the Northeast coast of Honshu (EMSC). The earthquake and the subsequent major tsunami caused huge losses in human lives, infrastructure and led to the Fukushima disaster. The World Bank estimated the total economic loss to be around US\$235 billion, labelling it as the costliest natural disaster in history (Kim, 2011). Thousands of aftershocks and over 80 above  $M_w 6.0$  were recorded in the following weeks and months. On the same day alone, three aftershocks of  $M_w 7.4$ ,  $7.9$  and  $7.1$  were recorded. 9 additional earthquakes over  $M_w 7.0$  were attributed as aftershocks as of March 2016 ("event page", USGS). The epicentre was located 130 km away from Sendai and roughly 135 km away from

Tono City and 115 km away from Kamaishi City and the shaking was described as severe (see Figure 4).

In these two towns, both North of Sendai, slope stabilisation measures were installed, both flexible high tensile steel wire mesh with soil nails and hard facing concrete structures. The pictures speak for themselves, the concrete grating cribs got severely damaged and dislocated from the slope whereas no slope movement was observed where the Tecco systems were installed (see Figures 5 to 7).



Figure 5: Collapse of shotcrete grating crib work in Kuji City after the earthquake. Buckling and shearing of the concrete ribs are observed.

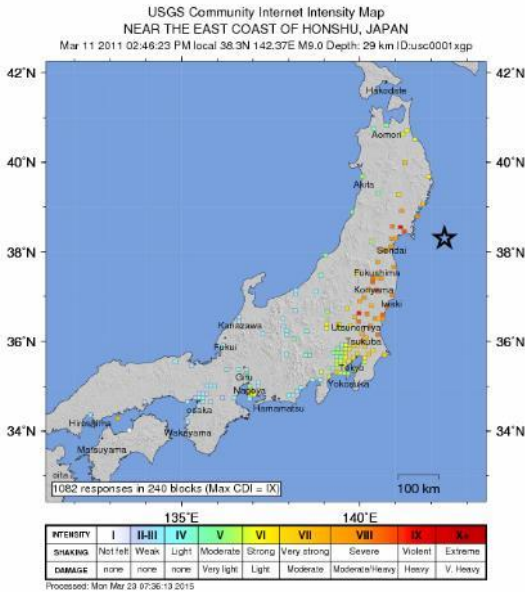


Figure 4: Intensity Map for the 9.1 earthquake near the E coast of Honshu Japan, on 11<sup>th</sup> of March 2011 (Poster, USGS).



Figure 6: Not far away, a stretch of road where the slope stabilization was done with high tensile steel flexible system and soil nailing and has long been re-vegetated, in Tono City. The whole stretch of slope along the road remained stable throughout the earthquake swarm.



Figure 7. Example of a more recent slope stabilisation project in Kamaishi City. The vegetation has not yet had the time to regrow. The devastation of the subsequent tsunami after the Tohoku earthquake is visible. In the background the slope remained stable, being stabilised with the Tecco system.

#### 4.2 United States; Hounds Ear, North Carolina

On August 23<sup>rd</sup>, 2011, the largest ever recorded earthquake in the eastern US occurred, in Louisa, Virginia (Poster, USGS). Ground shaking is felt across a large area with reports across neighbouring states such as the example in Hounds Ear, North Carolina (see Figure 8). Intensity was described as light to moderate. Prior the earthquake an unstable rock slope was discovered during the renovation of a carport. Slope stabilisation was performed with high tensile steel wire mesh and soil nails before continuing the work on the carport. The slope remained stable during the earthquake (see Figure 9).

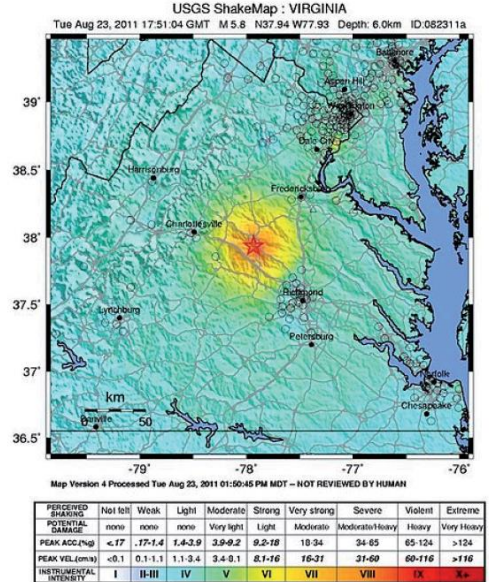


Figure 8: Intensity Map after the 5.8 earthquake close to Louisa, Virginia, US (Poster, USGS)



Figure 9: Slope stabilisation under a newly built residential car park. No damages were observed during and after the earthquake. The potential damage of slope failure would have resulted in the collapse of the residential compound and the car park.

#### 4.3 Chile; Caleta Tumbes, Talcahuano

On February 27, 2010, a magnitude 8.8 earthquake struck just off the coast close to the city of Concepción, in Chile (Poster, USGS). The intensity described was violent (see Figure 10).

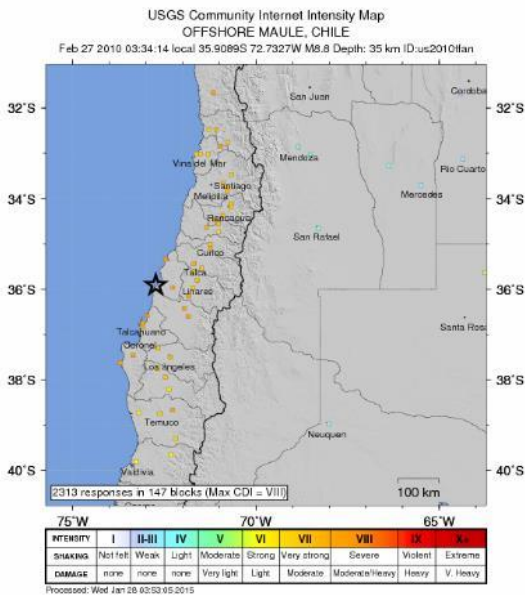


Figure 10: Intensity map after the 8.8 Bio-Bio earthquake, offshore of the coast of Chile (Poster, USGS).

Concepción and Talcahuano where the slope remediation is situated, were only 70km away from the epicentre. A subsequent tsunami devastated several coastal towns, including the harbour of Talcahuano and even reached the Tohoku region in Japan, just a year before their 9.1 earthquake. The losses to the Chilean economy was estimated at US\$15-30 billion (see Figure 11).



Figure 11: Damage in Caleta Tumbes, Talcahuano after the earthquake.

Slope stabilisation works in Caleta Tumbes, were started end of 2009 with the Tecco system

and was just finished in time to prevent a large slope failure adding to the already severe damage of the surroundings (see Figure 12 and 13).



Figure 12: Previously installed Tecco system, which did not sustain any damage during and after the earthquake. The slope remained stable.



Figure 13: Overview of the stabilised road stretch being. No deformation or failure after the earthquake.

## 5 CONCLUSIONS

The worldwide experience in the last 8 years presented in this paper show the adaptability of Tecco to withstand large magnitude earthquakes, preventing already unstable slopes to fail. The recent  $M_w$ 6.8 earthquake in the Ionian Sea, just adds up now to an additional example of successful slope retention by flexible high tensile

steel mesh. More information is not available yet but might be presented at the conference.

Following the M7.8 Kaikoura earthquake in New Zealand in 2016, several slope stabilisations with Tecco system were installed., They in comparison to the other case studies have not been tested yet, but will probably soon. As with the previous examples and the correct dimensioning with RUVOLUM the slopes should stay stable this time.

## 6 REFERENCES

[EN14490]

DIN EN 14490:2010-11 Execution of special geotechnical works – Soil nailing; english translation; DIN Deutsches Institut für Normung e.V. Berlin. Beuth Verlag GmbH.

Allen, T.I., Wald, D.J., Hotovec, A.J., Lin, K., Earle, P.S. and Marano, K.D., 2008, An Atlas of ShakeMaps for Selected

Global Earthquakes: U.S. Geological Survey Open-File Report 2008–1236, 35 p

Bolt, B. A. (2018, August 23). Earthquake. Retrieved August 29, 2018, from <https://www.britannica.com/science/earthquake-geology/Surface-phenomena>

Cala M., Flum D., Roduner A., Rügger R., Wartmann S., (2012), TECCO (R) Slope Stabilization System and RUVOLUM (R) Dimensioning Method. Romanshorn, Switzerland: Beltz Bad Langensalza GmbH

Clague J., Stead D., (2012), Landslides Types and Mechanisms and Modelling. Cambridge, UK: Cambridge University Press 2012

Event page. Retrieved August 29, 2018, from [https://earthquake.usgs.gov/earthquakes/eventpage/official20110311054624120\\_30/executive](https://earthquake.usgs.gov/earthquakes/eventpage/official20110311054624120_30/executive)

GSHAP, ETHZ. Retrieved August 29, 2018, from <http://static.seismo.ethz.ch/GSHAP/global/>

Kim, V (21 March 2011). "Japan damage could reach \$235 billion, World Bank estimates". Los Angeles Times. Archived from the original on 12 April 2011. Retrieved 21 March 2011.

Mw 9.0 off the Pacific coast of Tohoku, Japan Earthquake, on March 11th, 2011 at 05:46 UTC. (n.d.). Retrieved August 29, 2018, from <https://www.emsc-csem.org/Earthquake/196/Mw-9-0-off-the-Pacific-coast-of-Tohoku-Japan-A-Earthquake-A-on-March-11th-2011-at-05-46-UTC>

“Nearly half americans exposed”. Retrieved August 29, 2018, from <https://www.usgs.gov/news/nearly-half-americans-exposed-potentially-damaging-earthquakes>

Poster M8.8 Maule Earthquake. Retrieved August 29, 2018, from <https://earthquake.usgs.gov/archive/product/poster/20100227/us/1510004584876/poster.jpg>

Poster The M9.0 Great Tohoku Earthquake. Retrieved August 29, 2018, from <https://earthquake.usgs.gov/archive/product/poster/usp000hvnu/us/1538164175255/poster.medium.jpg>

Poster M5.8 Central Virginia Earthquake of 23 August 2011. Retrieved August 29, 2018, from <https://earthquake.usgs.gov/archive/product/poster/20110823b/us/1484858447780/poster.jpg>

“seismic hazards central Virginia”. Retrieved August 29, 2018, from

Slope stabilisation in earthquake prone environment – with a flexible high tensile steel chain-link mesh

[https://www.usgs.gov/centers/fbgc/science/geologic-framework-seismic-hazards-central-virginia?qt-science\\_center\\_objects=0#qt-science\\_center\\_objects](https://www.usgs.gov/centers/fbgc/science/geologic-framework-seismic-hazards-central-virginia?qt-science_center_objects=0#qt-science_center_objects)

USGS updates National Seismic Hazard Maps. (2014, July 30). Retrieved August 29, 2018, from <https://www.bdcnetwork.com/usgs-updates-national-seismic-hazard-maps>